

DTIC FILE COPY

4

MEMORANDUM REPORT BRL-MR-3708

**BRL**

1938 - Serving the Army for Fifty Years - 1988

AD-A201 107

GROUND TESTING FOR BASE-BURN PROJECTILE SYSTEMS

LYLE D. KAYSER  
JOHN D. KUZAN  
DAVID N. VAZQUEZ

NOVEMBER 1988

DTIC  
ELECTE  
NOV 21 1988  
S D  
CGH

APPROVED FOR PUBLIC RELEASE; DISTRIBUTION UNLIMITED.

U.S. ARMY LABORATORY COMMAND

**BALLISTIC RESEARCH LABORATORY**  
**ABERDEEN PROVING GROUND, MARYLAND**

DESTRUCTION NOTICE

Destroy this report when it is no longer needed. DO NOT return it to the originator.

Additional copies of this report may be obtained from the National Technical Information Service, U.S. Department of Commerce, Springfield, VA 22161.

The findings of this report are not to be construed as an official Department of the Army position, unless so designated by other authorized documents.

The use of trade names or manufacturers' names in this report does not constitute indorsement of any commercial product.

UNCLASSIFIED

SECURITY CLASSIFICATION OF THIS PAGE

## REPORT DOCUMENTATION PAGE

Form Approved  
OMB No. 0704-0188

1a. REPORT SECURITY CLASSIFICATION <b>UNCLASSIFIED</b>			1b. RESTRICTIVE MARKINGS		
2a. SECURITY CLASSIFICATION AUTHORITY			3. DISTRIBUTION/AVAILABILITY OF REPORT Approved for public release; distribution is unlimited.		
2b. DECLASSIFICATION/DOWNGRADING SCHEDULE			5. MONITORING ORGANIZATION REPORT NUMBER(S)		
4. PERFORMING ORGANIZATION REPORT NUMBER(S) <b>BRL-MR-3708</b>			7a. NAME OF MONITORING ORGANIZATION		
6a. NAME OF PERFORMING ORGANIZATION <b>U.S. Army Ballistic Research Laboratory</b>		6b. OFFICE SYMBOL (If applicable) <b>SLCBR-LF</b>	7b. ADDRESS (City, State, and ZIP Code)		
6c. ADDRESS (City, State, and ZIP Code) <b>Aberdeen Proving Ground, MD 21005-5066</b>			9. PROCUREMENT INSTRUMENT IDENTIFICATION NUMBER		
8a. NAME OF FUNDING/SPONSORING ORGANIZATION <b>U.S. Army Ballistic Research Laboratory</b>		8b. OFFICE SYMBOL (If applicable) <b>SLCBR-DD-T</b>	10. SOURCE OF FUNDING NUMBERS		
8c. ADDRESS (City, State, and ZIP Code) <b>Aberdeen Proving Ground, MD 21005-5066</b>			PROGRAM ELEMENT NO. <b>62618A</b>	PROJECT NO. <b>IL1 62618AH80</b>	TASK NO. <b>WORK UNIT ACCESSION NO.</b>
11. TITLE (Include Security Classification) <b>Ground Testing for Base Burn Projectile Systems (U)</b>					
12. PERSONAL AUTHOR(S) <b>Kayser, Lyle D.; Kuzan, John D.; and Vazquez, David N.</b>					
13a. TYPE OF REPORT <b>Memorandum Report</b>		13b. TIME COVERED FROM _____ TO _____		14. DATE OF REPORT (Year, Month, Day) <b>1988 July</b>	
15. PAGE COUNT <b>32</b>					
16. SUPPLEMENTARY NOTATION					
17. COSATI CODES			18. SUBJECT TERMS (Continue on reverse if necessary and identify by block number)		
FIELD	GROUP	SUB-GROUP			
<b>01</b>	<b>01</b>		<b>&gt;Base Burn Projectile Spin Fixture. Chamber Pressure.</b>		
19. ABSTRACT (Continue on reverse if necessary and identify by block number)					
<p>A ground test spin fixture was used to obtain measurements in the base region of a 155mm M864 projectile. The M864 uses the base burn concept of reducing base drag by injecting gas, generated by burning propellant, into the base area. Pressure and temperature measurements were obtained in the base area of the projectile, with the base burn active, at spin rates up to 250 rps. Data illustrate that increased spin rate increases the pressure in the propellant chamber and increases substantially the burning rate of the propellant. The ground tests provided information on measurement techniques which will be used in free-flight experiments.</p>					
20. DISTRIBUTION/AVAILABILITY OF ABSTRACT <input type="checkbox"/> UNCLASSIFIED/UNLIMITED <input checked="" type="checkbox"/> SAME AS RPT. <input type="checkbox"/> DTIC USERS			21. ABSTRACT SECURITY CLASSIFICATION <b>UNCLASSIFIED</b>		
22a. NAME OF RESPONSIBLE INDIVIDUAL <b>Lyle D. Kayser</b>			22b. TELEPHONE (Include Area Code) <b>(301)-278-3815</b>		22c. OFFICE SYMBOL <b>SLCBR-LF-A</b>

## Acknowledgments

Martin Miller and William McBratney of the Interior Ballistics Division provided the pyrotechnic expertise for motor ignition, the video coverage, and other professional assistance essential to the test program.



Accession For	
NTIS GRA&I	<input checked="checked" type="checkbox"/>
DTIC TAB	<input type="checkbox"/>
Unannounced	<input type="checkbox"/>
Justification	
By	
Distribution/	
Availability Codes	
Avail and/or	
Dist	Special
A-1	

## Table of Contents

	<u>Page</u>
List of Tables . . . . .	vii
List of Figures . . . . .	ix
I. Introduction . . . . .	1
II. Experiment . . . . .	2
1. Apparatus . . . . .	2
2. Test Set-Up and Data Acquisition Procedure . . . . .	6
3. Test Run Summary . . . . .	10
4. Data Reduction . . . . .	10
III. Results . . . . .	13
IV. Analysis and Discussion . . . . .	24
V. Conclusions . . . . .	28
Distribution List . . . . .	29

## List of Tables

<u>Table</u>		<u>Page</u>
1	Recorded Data for Phase I and II . . . . .	8
2	Test Run Summary . . . . .	11
3	Equivalent Burn Time . . . . .	24

## List of Figures

<u>Figure</u>		<u>Page</u>
1	Spin Fixture Photograph . . . . .	3
2	Transducers and Mounting Fixture Photograph . . . . .	4
3	Circuit Board Photograph . . . . .	5
4	Base and Instrument Canister Assembly . . . . .	7
5	Alignment Set Screws . . . . .	8
6	Propellant Grain Geometry . . . . .	9
7	Base, Propellant, and Igniter for AP-2 Propellant Tests . . . . .	10
8	Igniter for AP-1 Propellant Tests . . . . .	11
9	Test Installation Photograph . . . . .	12
10	Photograph of Base During AP-2 Propellant Test . . . . .	14
11	Effect of Spin Rate on the Length of Propellant Burn . . . . .	16
12	Ignition and Early Pressure History for AP-1 Propellant . . . . .	17
13	Chamber Pressures for AP-1 Propellant Tests . . . . .	18
14	Effects of Spin Rate on Chamber Pressure, AP-2 Propellant . . . . .	19
15	Chamber Pressure Fluctuations, AP-2 Propellant . . . . .	20
16	Ignition Phase of Propellant Burn, AP-2 Propellant . . . . .	21
17	Early Chamber Pressure History, AP-2 Propellant . . . . .	22
18	Chamber Temperature Measurements, AP-2 Propellant . . . . .	23
19	Estimated Mass Flow Rates vs. Measured Chamber Pressure . . . . .	25
20	Estimated Gas Densities in the Base Throat . . . . .	26
21	Estimated Throat Velocities . . . . .	27

## I. Introduction

Low velocity injection of mass into the wake region of a projectile reduces the base drag on the projectile. Since base drag may account for one half of the total drag on a projectile, substantial reductions in base drag equate to substantial increases in the range of the artillery system. The base burn concept is to provide mass injection by burning propellant housed in the base of the projectile. This housing is referred to as the propellant chamber and the mass injection occurs through a hole in the chamber. The hole is not a nozzle, such as that found in a rocket-assisted projectile, so that the thrust resulting from the burning propellant is small.

Accurate measurements and numerical models are uncommon for base flows, owing to their complexity; hence, systems which reduce base drag are difficult to design. In spite of this, the 155mm M864 uses a base burn system successfully for extending its range. However, modeling efforts and system performance would benefit from in-flight measurements of temperature and pressure in the projectile propellant chamber and base region.

Certain problems exist which make design of such an in-flight measurement system difficult. It was realized that many of these problems could be addressed using a spinning ground test fixture. Therefore, the objectives of the current effort were: (1) to build a spinning ground test fixture, (2) to obtain performance characteristics of burning propellants, and (3) to examine techniques which could be applied to telemetry instrumented free-flight projectiles. Since propellant burning occurs outside of the gun tube and lasts for a considerable portion of the total flight, the inability to simulate launch conditions was not a serious deficiency in ground testing. Ground tests simulated spin rates up to 250 rps (15,000 rpm) which are typical of an 155mm projectile launched at maximum velocity. Also, in consideration of the second objective, variations in altitude over the projectile trajectory dictate the need for testing in a variety of ambient pressures.

The resulting fixture weighs approximately 50 kg and has dimensions of one-half meter by one meter by one-third meter high. It holds a projectile base and propellant combination and is spun by an air motor. The propellant was in a monolithic form and, as such, will be referred to as the propellant grain. The design of the instrumentation system was based upon flight tests where forebody and transonic surface pressures were measured successfully and compared to computed data.<sup>1</sup> For the ground tests, data signals were transmitted across a slip ring assembly rather than by telemetry, as required in free flight.

The results presented were obtained at sea level atmospheric pressure. Facilities are available for conducting tests at lower pressures.

This work was supported by the Project Manager, Cannon Artillery Weapon Systems (PMCAWS) and the U.S. Army Research Development and Engineering Center (ARDEC), Picatinny Arsenal, New Jersey.

<sup>1</sup> Kayser, L.D., Clay W.P., D'Amico W.P., "Surface Pressure Measurements on 155mm Projectile in Free-Flight at Transonic Speeds," ARBRL-MR-3534, Ballistic Research Laboratory Memorandum Report No. 3534, July 1986.



## II. Experiment

### 1. Apparatus

A photograph of the spin fixture is shown in Figure 1. The rotor is supported by a set of duplex bearings at the two pedestal locations. The bearings have a bore diameter of 30.0 mm, an outside diameter of 55.1 mm, and are rated for speeds in excess of 20,000 rpm. The M864 projectile base and instrumentation canister are seen on the left side of the photograph. An air motor is mounted on the pedestal between the two bearing supports. Nitrogen is brought into a plenum through the tube fittings and is then directed toward the turbine blades through four small nozzles. Signal leads pass from the canister through the rotor shaft and are connected to the slip ring assembly which is on the far right of the photograph.

A balancing disc with threaded holes is located near the slip ring. Balancing holes are also placed in one end of the canister, thus, permitting two-plane dynamic balancing of the rotor. Two follower-type rollers were mounted near the canister to constrain the amplitude of vibration in the event a severe resonance was encountered. Without the presence of a propellant grain, a fundamental resonant frequency of 79 Hz and a harmonic of 350 Hz were found to exist in the spin fixture.

The pressure transducers used in these experiments were purchased from the Kulite Corporation and are miniature, solid-state semiconductor strain-gage sensors with a four element bridge circuit. Figure 2 shows the transducer fixture with one transducer inserted and another transducer not installed. The transducer is equipped with a 10-32 UNF thread and an O-ring making it convenient for installation. The transducers are rated for 25 psia full scale; however, they are equipped with mechanical stops for an overload protection of 40 times the rated pressure. The transducer sensitivity to acceleration is very low and is quoted to be typically 0.0005% of full scale per "g" perpendicular to the diaphragm and 0.0001% transverse to the diaphragm.

A hole was drilled through the transducer fixture and the base so that a thermocouple could be inserted into the propellant chamber. A tungsten, tungsten-rhenium thermocouple was used to measure temperature inside the propellant chamber. A slightly non-constant cold junction temperature of approximately 80° F inside the instrumentation canister was considered adequate for the relatively high temperatures to be measured.

The three channel circuit board shown in Figure 3 was mounted inside the instrumentation canister approximately 20 mm above the transducers. Power to the circuit board was supplied across the slip rings. The board contained a voltage regulator which supplied power to the transducers. Output from the transducers was amplified by a factor of approximately 30. A timer and switching device which shorted the output of the gages for 10 msec at 12 sec intervals was also provided in the circuit. The primary purpose in shorting the gages was to track any zero shift in the circuit. This feature was included primarily for the planned free-flight tests but was also useful in the ground tests. Centrifugal

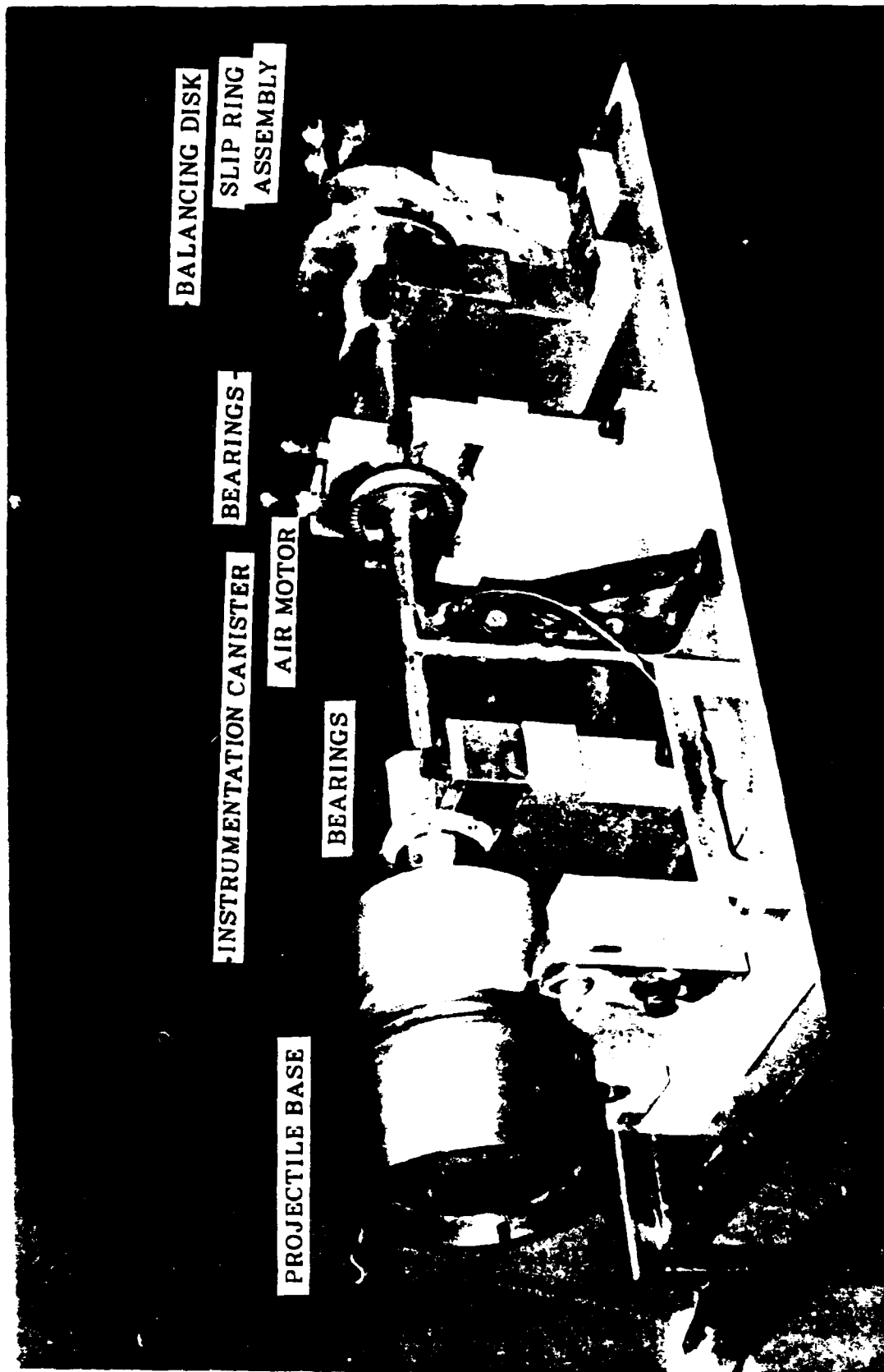


Figure 1. Spin Fixture Photograph

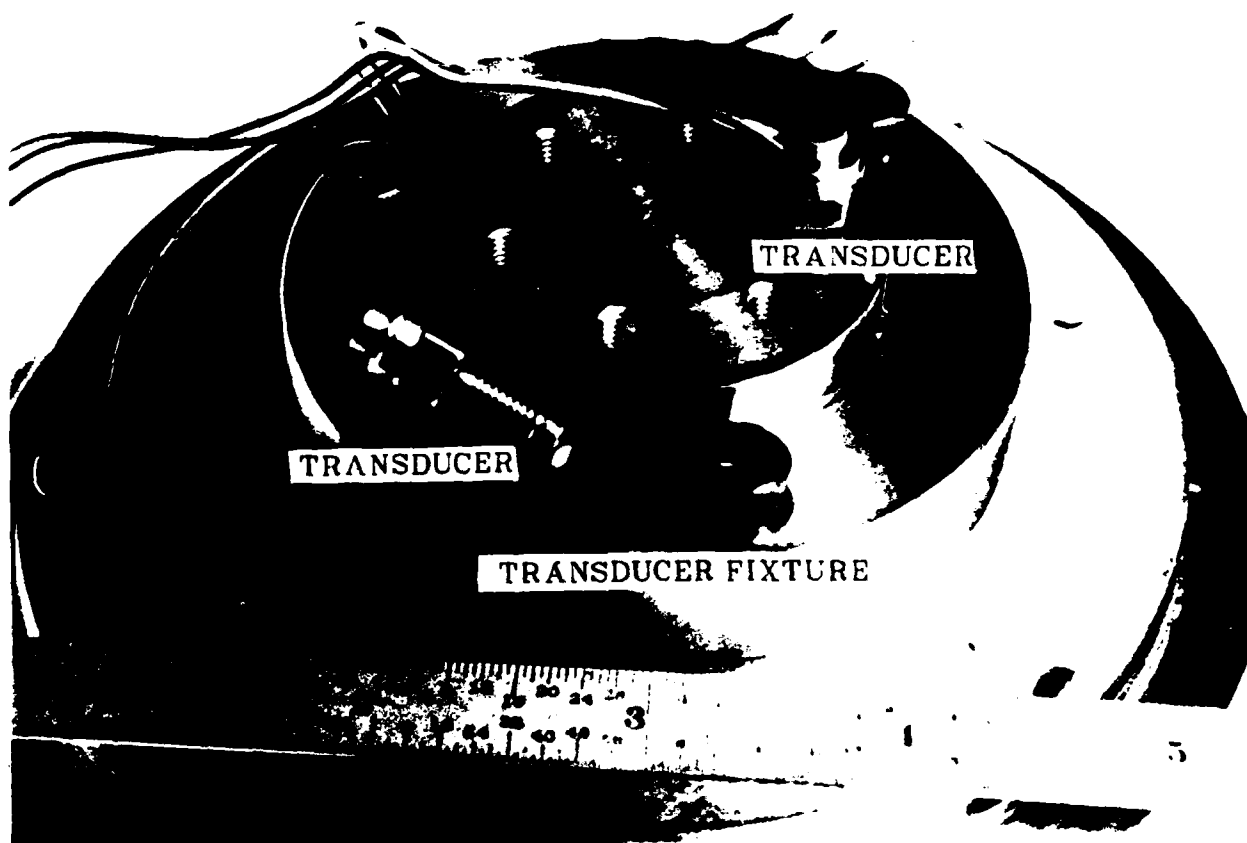


Figure 2. Transducers and Mounting Fixture Photograph

acceleration forces caused drastic failures in the electronics. It was found that filling the voided areas of the instrumentation canister with small (0.3mm) glass beads adequately supported the electronic components at 15,000 rpm.

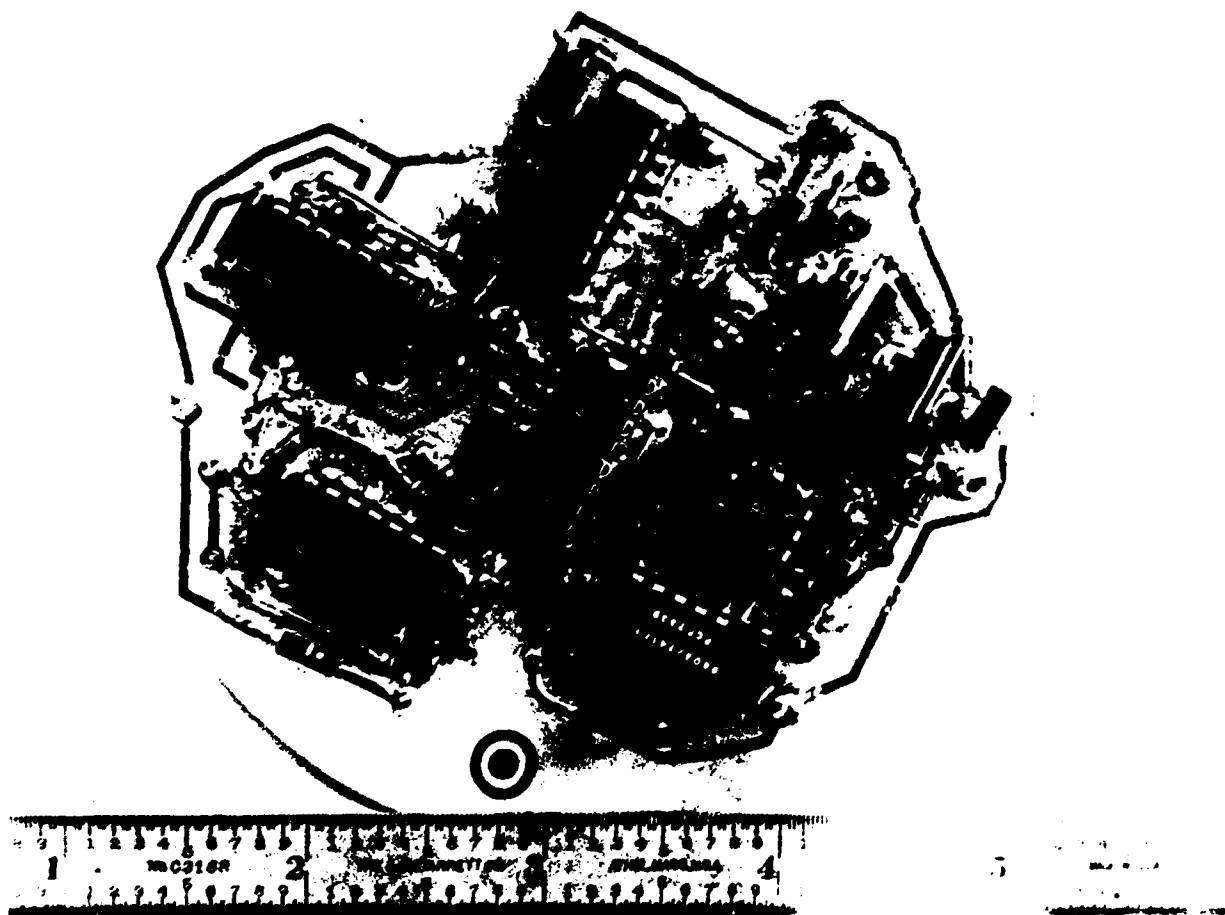


Figure 3. Circuit Board Photograph

A Lebow Products, Eaton Corporation slip ring assembly, rated at 8,000 rpm continuous use, was used to acquire data signals from the rotating payload. The slip ring assembly contained 12 epoxy-embedded coin silver slip rings. Two silver graphite brushes, which were easily replaceable, made contact with each of the rotating rings.

A Kaman proximity motion sensor, which uses the eddy current operating principle, was placed near the rotating shaft. The output was monitored with an oscilloscope, and small increases in system vibration were readily detectable. A Scan-O-Matic reflective detector was placed near the balancing disc; output was visually monitored by a frequency counter and used for controlling the spin rate.

Figure 4 is a sketch of the 155mm M864 base and instrumentation canister. It shows the paths provided for pressure at the base area to be sensed at the transducers. Holes of 2.0mm (5/64 inch) diameter were drilled in several segments with split point drills.

Sections of the holes were then plugged by welding to provide a leak free path from the orifice opening to the transducer. A leak free path was achieved across the threaded joint of the two base halves through careful alignment of the holes and the use of small O-ring seals. The alignment was secured by placing three set screws through the threaded section at circumferential positions between the pressure paths, as shown in Figure 5. Figure 4 also shows the location of the different orifice positions and the circumferential locations; Figure 4 is not a true cross sectional view.

The testing was conducted in two phases which involved the use of two different propellant grains. The standard M864 propellant grain, designated as AP-2, was used for the second phase of testing and its geometry is shown in figure 6. An inhibitor of approximately one mm thickness is bonded to the outer periphery of the grain so that burning is limited to the central core and to the slotted areas. The first phase of the test program utilized a non-standard, faster burning formulation, AP-1, because the standard grain was not available at that time. The AP-1 grain was similar in geometry, except for different hole diameters.

Figure 7 shows the projectile base with the propellant and the propellant igniter housing in place and the ignition apparatus for the AP-2 phase of the testing. Three grams of black powder were placed in an external igniting apparatus. An additional gram of black powder was cemented to the surface of the propellant grain. A modified igniter housing and ignition apparatus for the AP-1 phase of the testing is shown in Figure 8. Power to ignite the electric match was supplied across the slip ring.

## **2. Test Set-Up and Data Acquisition Procedure**

Figure 9 is a photograph that shows the spin fixture installed in a test chamber at the Interior Ballistics Division of the U.S. Army Ballistic Research Laboratory. The test chamber is equipped with a large exhaust fan that was used for quick removal of the propellant gasses. The photograph shows the base closure removed; the remains of a propellant liner and other residue are visible. After each burn, the propellant chamber was cleaned prior to installing another propellant grain.

For the AP-1 tests, the electric match leads were spot welded to molybdenum wires coming through the base as shown in Figure 8. The propellant grain was installed so that the gap between the propellant grain halves was aligned with the propellant chamber pressure orifice; the base closure was then installed.

For the AP-2 tests, one magnesium-teflon igniter was placed inside the igniter housing shown in Figure 7. The grain was then installed and the external ignition device, shown in Figure 7, was positioned. The test chamber was secured and data acquisition could begin.

Two high pressure (3,100 psi) nitrogen bottles were manifolded together, and nitrogen was supplied to the plenum of the air motor. The pressure at the air motor turbine blades was held at 200 psi until the rotor approached the desired spin rate. At that time the pressure was decreased to maintain the desired spin rate. Pressure was controlled manually with the hand valves on the nitrogen bottles, and rotor speed was held constant to within

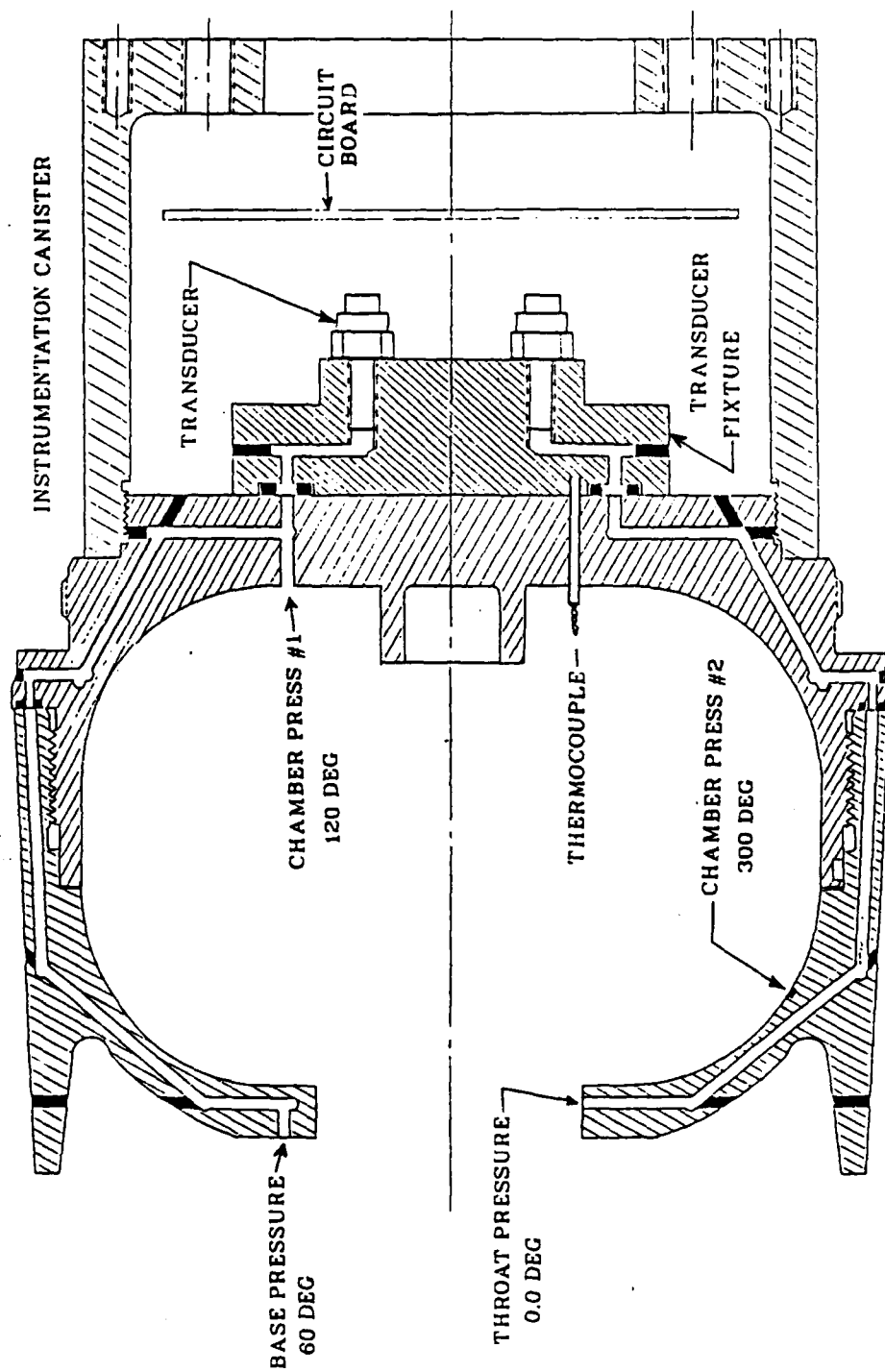


Figure 4. Base and Instrument Canister Assembly

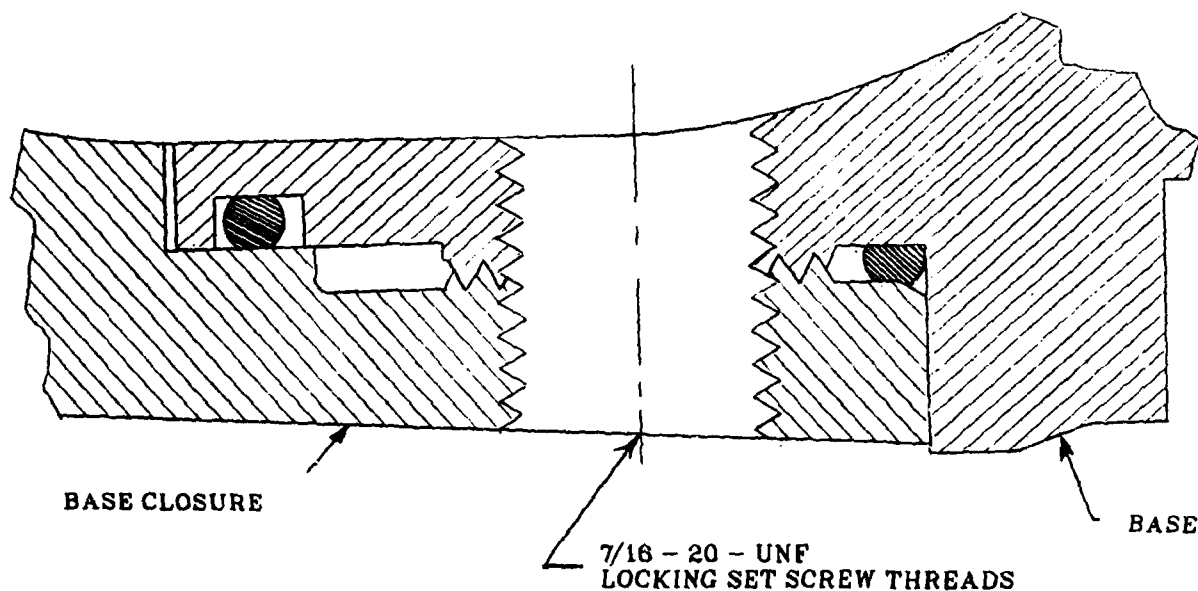


Figure 5. Alignment Set Screws

two rps. A spin-up time of about 70 seconds was required to bring the rotor up to 15,000 rpm (250 rps).

The propellant was ignited by applying a 20-volt pulse to the electric match that ignited the black powder which then ignited the propellant grain. Data recording on a Honeywell 101 analog tape recorder commenced with the start of spin-up and continued during the burning phase and for most of the spin-down period. A video camera, supplied by the Interior Ballistics Division, recorded the burning phase of the test. Table 1 shows data recorded on magnetic tape for both phases of the test.

Table 1. Recorded Data for Phase I and II

Phase I, AP-1 Propellant	Phase II, AP-2 Propellant
1. Throat pressure, 0 DEG	1. Chamber temperature, 210 DEG
2. Chamber pressure, 300 DEG	2. Chamber pressure #1, 120 DEG
3. Base pressure, 60 DEG	3. Chamber pressure #2, 300 DEG
4. Motion Sensor	4. Motion Sensor
5. Scan-O-Matic, rps	5. Scan-O-Matic, rps
6. Ignition pulse	6. Ignition Pulse

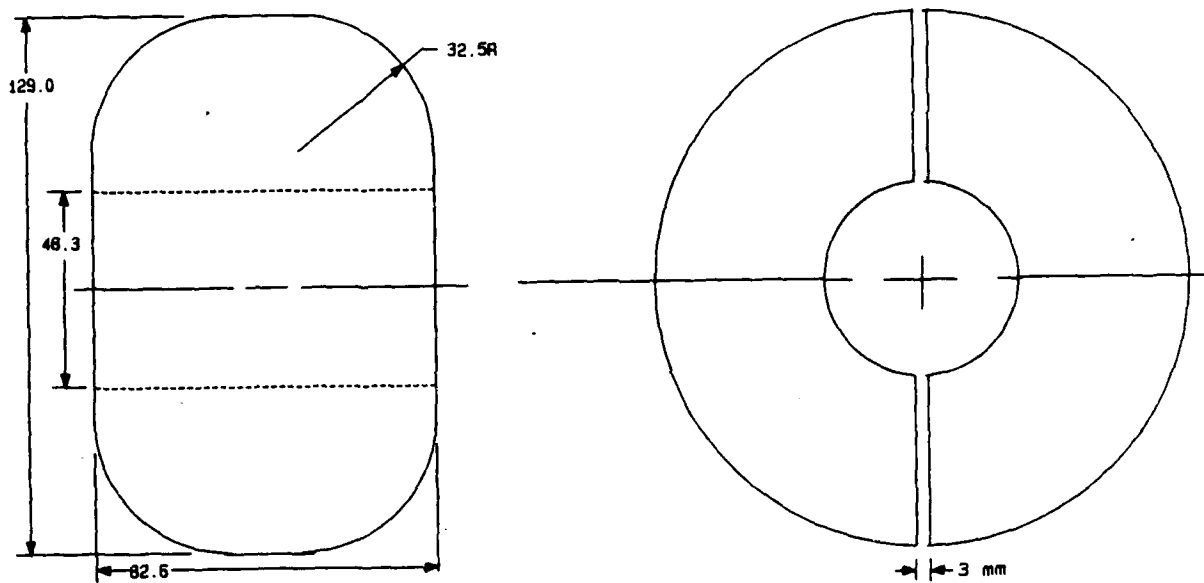
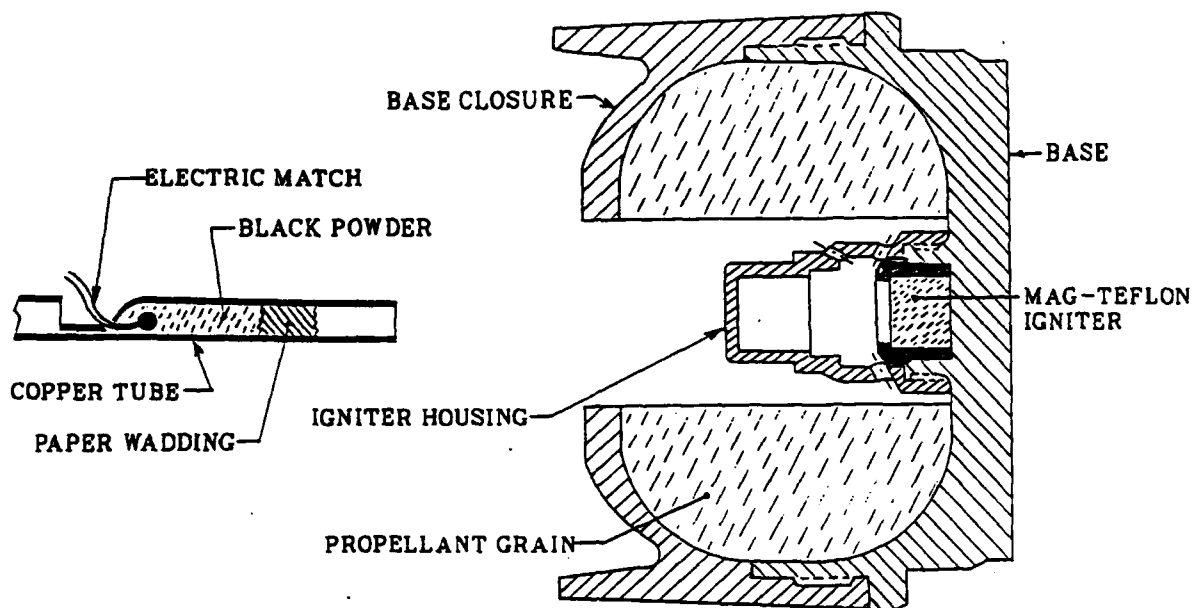


Figure 6. Propellant Grain Geometry





**Figure 7. Base, Propellant, and Igniter for AP-2 Propellant Tests**

### **3. Test Run Summary**

A summary of the test runs is given in Table 2. The first phase of testing used five AP-1 propellant grains which had the faster burning formulation and in the second phase of the test program, seven of the AP-2 propellant grains were burned. Notice that the hole size (inside diameter, ID) varied for some of the grains. From Table 1, it can be seen that the basic measurements involving channels 1,2, and 3 are different for the two test phases. During the first phase, the throat pressure orifice often became plugged or if it was not plugged the measured pressure was very close to ambient. Also during the first test phase, the base pressure was found to be equal to the ambient pressure. For the second phase of testing, a temperature measurement was substituted for the throat pressure and an additional chamber pressure was substituted for the base pressure.

### **4. Data Reduction**

The analog signals, initially recorded on one-inch magnetic tape, were digitized at 500 samples per second by a Digital AD11-K analog-to-digital converter and were stored on a Digital VAX 11-730 computer. The analog-to-digital converter was controlled using Signal Technology's Interactive Laboratory System software. Analog signal conditioning was performed with a Precision Filters Model 32 Programmable Multi-Channel Filter System in order to low-pass filter the signal at 400 Hertz and to impart a gain of 5 to the

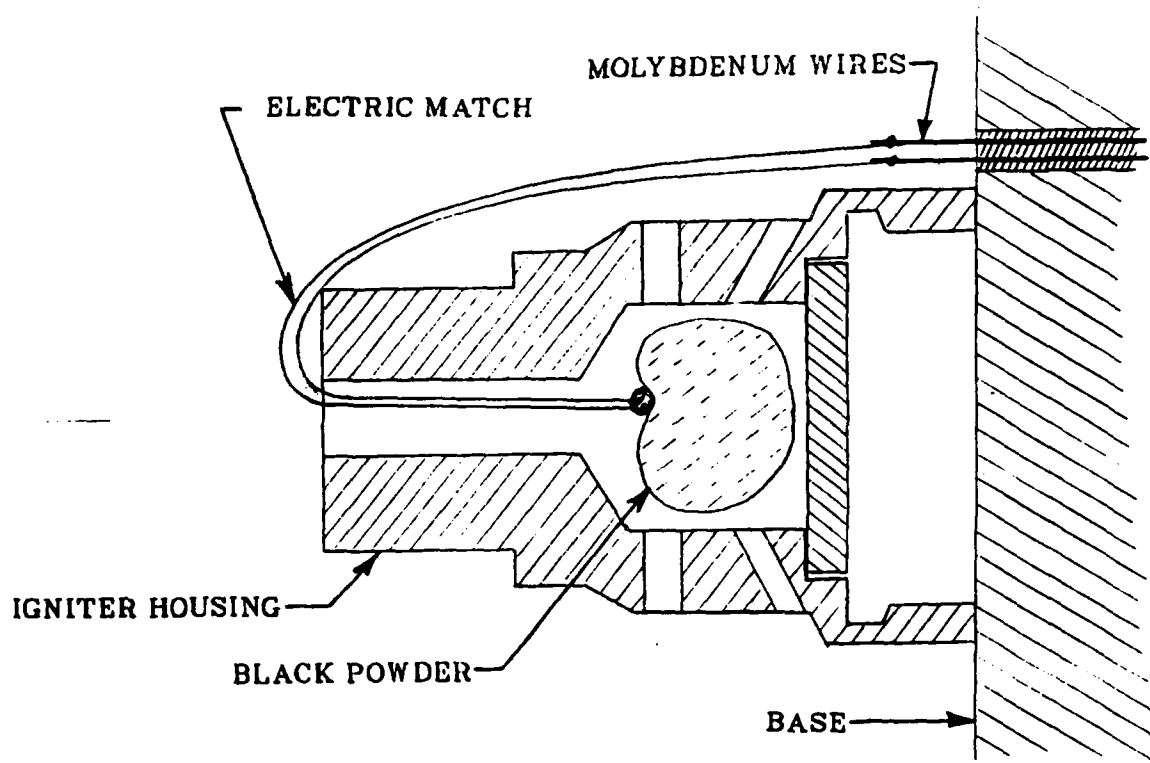
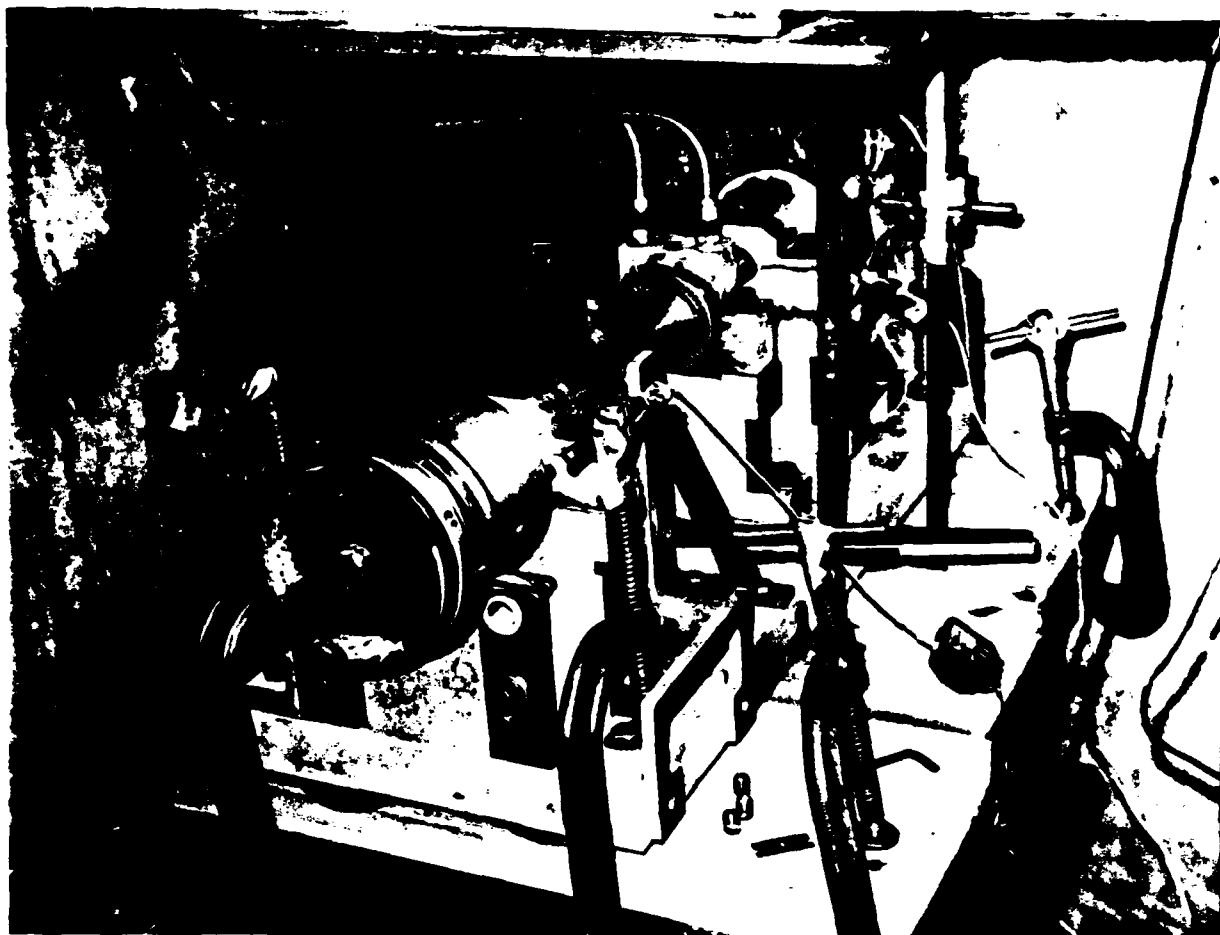


Figure 8. Igniter for AP-1 Propellant Tests

Table 2. Test Run Summary

Phase I, AP-1 Propellant				
Run	RPS	ID (mm)	Burn Time (sec)	Comment
1	55	41	23.4	-
2	133	53	16.1	-
3	133	41	21.5	instrument failure
4	115	41	22.4	-
5	0	41	23.8	-
Phase II, AP-2 Propellant				
1	0	48	-	ignition failure
2	0	48	40.0	mag-teflon did not burn
3	99	48	31.9	electronic failure, also mag-teflon did not burn
4	142	48	29.0	-
5	176	48	27.4	-
6	199	48	26.0	-
7	226	48	23.9	-
8	253	48	22.8	-



**Figure 9.** Test Installation Photograph

signal. Prior to low-pass filtering, the analog pressure signal was offset to a value between 0 and 1 volt with a Tektronix model AM 502 Differential Amplifier. Pressure data were normalized with the local atmospheric pressure.

### III. Results

The presented results include the propellant chamber pressure, propellant chamber temperature, and the effect of spin rate on the time of propellant burn. The base pressure and throat pressure, obtained during the first phase of testing (AP-1 tests), did not differ significantly from ambient pressure and therefore are not presented. The AP-1 tests were limited to 8,000 rpm, as dictated by the slip ring design; but it was believed that higher spin rates would be possible for short duration experiments. Several spin excursions, up to 15,000 rpm, have been made without any noticeable slip ring problems.

Five of the AP-1 grains and seven of the AP-2 grains were burned in both phases of the tests. The propellant grain for run number two of the AP-1 phase was unique in geometry, i.e. a larger hole diameter, and therefore not useful for comparison to the other AP-1 grains. Also, no data were obtained for run number three which leaves three AP-1 tests at 0.0, 55, and 115 rps for comparisons. No data were obtained for the 100 rps run of the AP-2 tests leaving six runs at spin rates of 0, 142, 176, 199, 226, and 253 rps for useful comparisons. (For the AP-2 propellant tests, one magnesium-teflon igniter was installed in the igniter housing, although the housing is designed to hold two igniters.) Figure 10 is a photograph of the base during an AP-2 propellant burn at zero spin rate. It shows a bright plume of flame, which indicates that some burning occurs outside of the propellant chamber. As spin rate increases the plume shortens and becomes broader.

Figure 11 presents the burn time of the AP-1 and AP-2 propellants plotted against the spin rate. The effect of increasing spin rate is shown to decrease the burning time substantially or, conversely, to increase the burning rate. The experiments were video taped and the time of burn was measured using both the video tape and the pressure data. The length of burn from video records was taken to be the time interval for which the exit flame could be seen. From the recorded data, time zero was the instant that the electrical pulse was applied to the electric match and the time of burn-out was the instant when the chamber pressure returned to ambient pressure. Subsequent data show that noticeable burning of the grain started about 0.2 second after the electrical initiation pulse. Burning, sufficient to cause pressure buildup, started at about 0.4 second. Note that no pressure or temperature data are available for the AP-2 propellant at 100 rps; however, a burn time was extracted from a video tape made of that experiment.

In contrast to the effects of spin rate on burn time presented here, there is apparently no need for a firing tables correction for spin effects<sup>2</sup>. A constant value of 32 seconds is used as the propellant burn time for all quadrant elevations and muzzle velocities fired. The range of spin rates, at launch, for flight tests are approximately equal to the four highest spin rates of the ground tests. The corresponding burn times for the ground tests

<sup>2</sup> Lieske, R. F., "Determination of Aerodynamic Drag and Exterior Ballistic Trajectory Simulation for the 155mm, DPICM, M864 Base-Burn Projectile," to be published as a Ballistic Research Laboratory Memorandum Report, 1968.



Figure 10. Photograph of Base During AP-2 Propellant Test

are in a fairly narrow range of about 23.5 to 27.5 sec. Since the flight trajectories involve increasing altitudes (lowering ambient pressures), burn times should be greater than the ground test values. The reason for the nearly constant burn time of 32 seconds cannot be readily explained but there may be compensating factors; for example, a higher launch velocity resulting in a higher spin rate could cause faster burning, but the higher launch velocity also increases the average altitude which would reduce the burning rate. This reasoning would apply for a constant quadrant elevation but static or ground tests would indicate that burn time should increase with increasing quadrant elevation for a given launch velocity.

The effects of spin rate are further demonstrated in subsequent figures which show the chamber pressure versus time for propellant formulations AP-1 and AP-2 at the different spin rates. Miller<sup>3</sup> measured burning rates of the propellant in a laboratory strand burning apparatus. Applying his data to the zero spin cases, burn times of 21.1 seconds for the AP-1 propellant and 41.9 seconds for the AP-2 propellant are predicted. This compares to the experimentally measured times of 23.8 seconds for AP-1 propellant and approximately 41 seconds for the AP-2 propellant. The experimental "time" could have been adjusted for the ignition and startup of propellant burn which would decrease the AP-2 "time" by about 1.5 sec and decrease the AP-1 "time" by about 0.3 sec. The agreement for the AP-2 is good but the agreement for the AP-1 is considered to be fair. It should be noted that conditions of measurement in the spin fixture are significantly different than those in the strand burner of Miller.

Figure 12 shows the early pressure history for the propellant formulation AP-1 which was ignited as described in section II. A 20 volt pulse was applied to the electric match at time zero and ignition of the black powder produced a pressure pulse that peaked at about 40 milliseconds (marked by the letter "A"). The pressure dropped toward ambient, but then increased as the propellant began to burn. There seems to be an effect of spin on this early history which is indicated by higher peaks in the pressure at lower spin rates.

Figure 13 shows the pressure histories for the three AP-1 propellant tests. After the first few seconds, the pressures do not differ substantially, although it is noted that the range of spin rates is much less than for the AP-2 tests. It appears that the pressure orifice was partially obstructed near the end of the burn for the 115 rps case. This partial plugging caused the pressure decay to be delayed and indicated a burn time of about 26 sec, but the video record indicated a burn time of 22.5 seconds which is believed to be correct.

The AP-2 propellant formulation results for chamber pressure, port number one, are shown in Figure 14. Severe plugging occurred in chamber pressure, port number two, and those results are not presented in this report. At low spin rates, the maximum chamber pressure occurs near the start of the propellant burn and decreases gradually to atmospheric pressure. As the spin rate is increased, the maximum chamber pressure occurs towards the end of propellant burn and the chamber pressure drops rapidly from this maximum to atmospheric pressure. The magnitude of the pressure fluctuations increases with increased spin rate. This is shown further in Figure 15 which gives the 0.5 Hz high

<sup>3</sup> M.S. Miller, H.E. Holmes, "An Experimental Determination of Sub-Atmospheric Burning Rates and Critical Combustion Diameters for AP-HTPB Propellant," *Proceedings of the 24th JANNAF Combustion Meeting*, October 1987

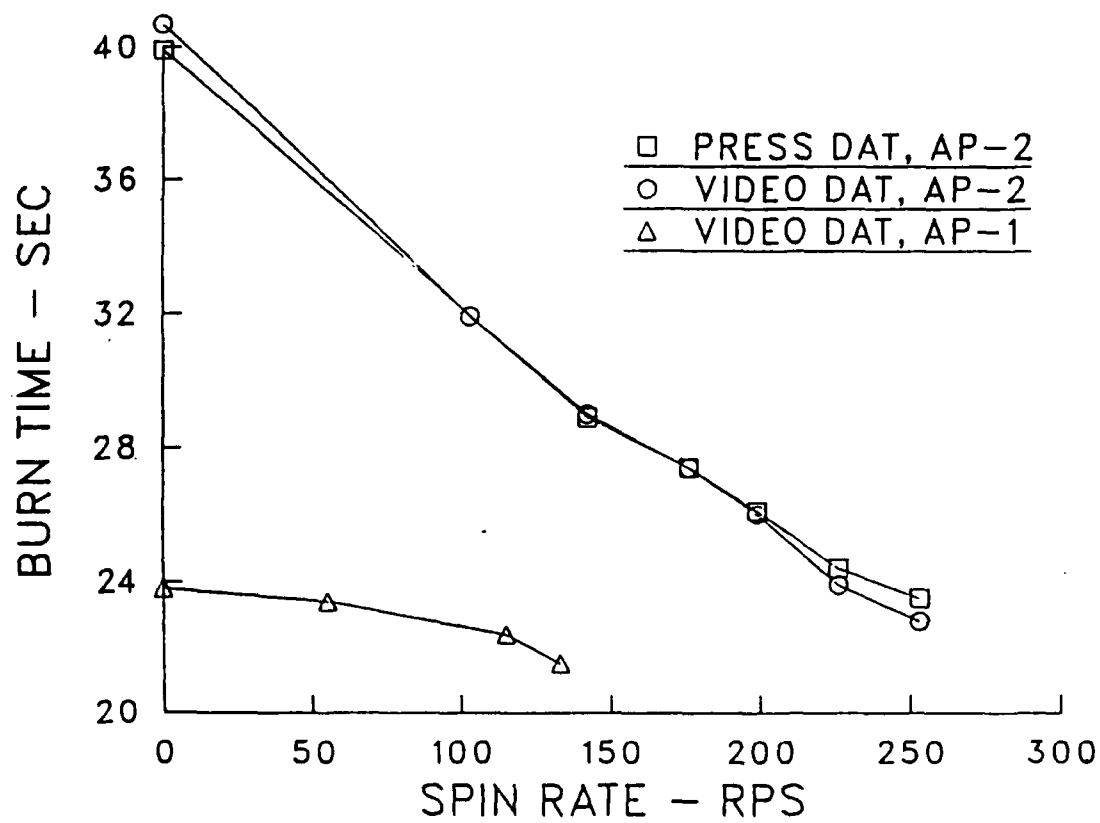


Figure 11. Effect of Spin Rate on the Length of Propellant Burn

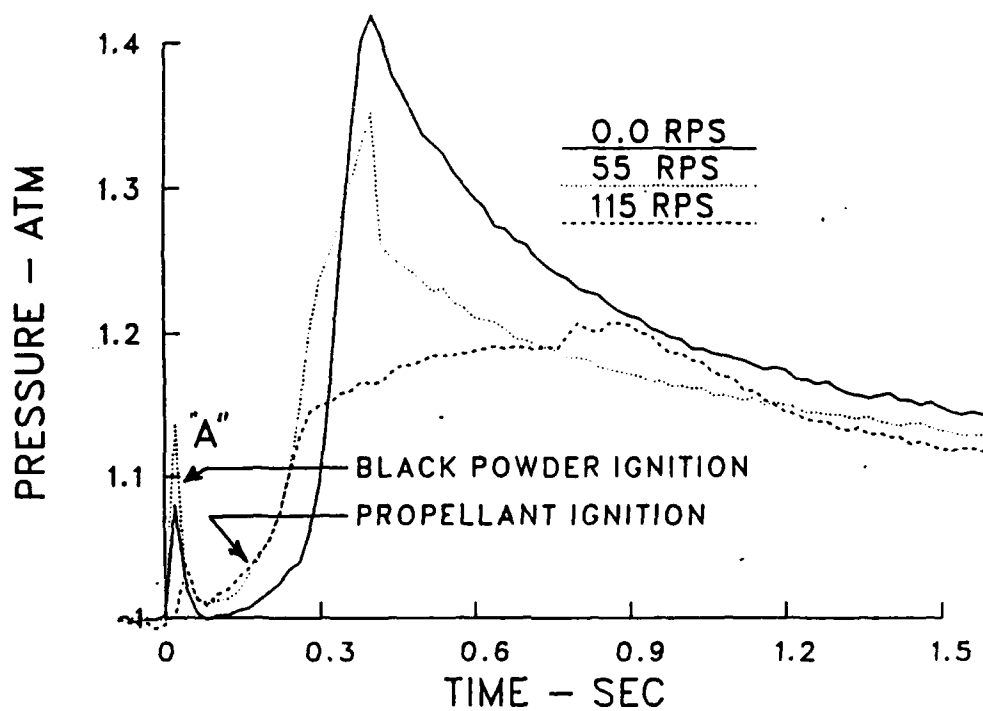


Figure 12. Ignition and Early Pressure History for AP-1 Propellant



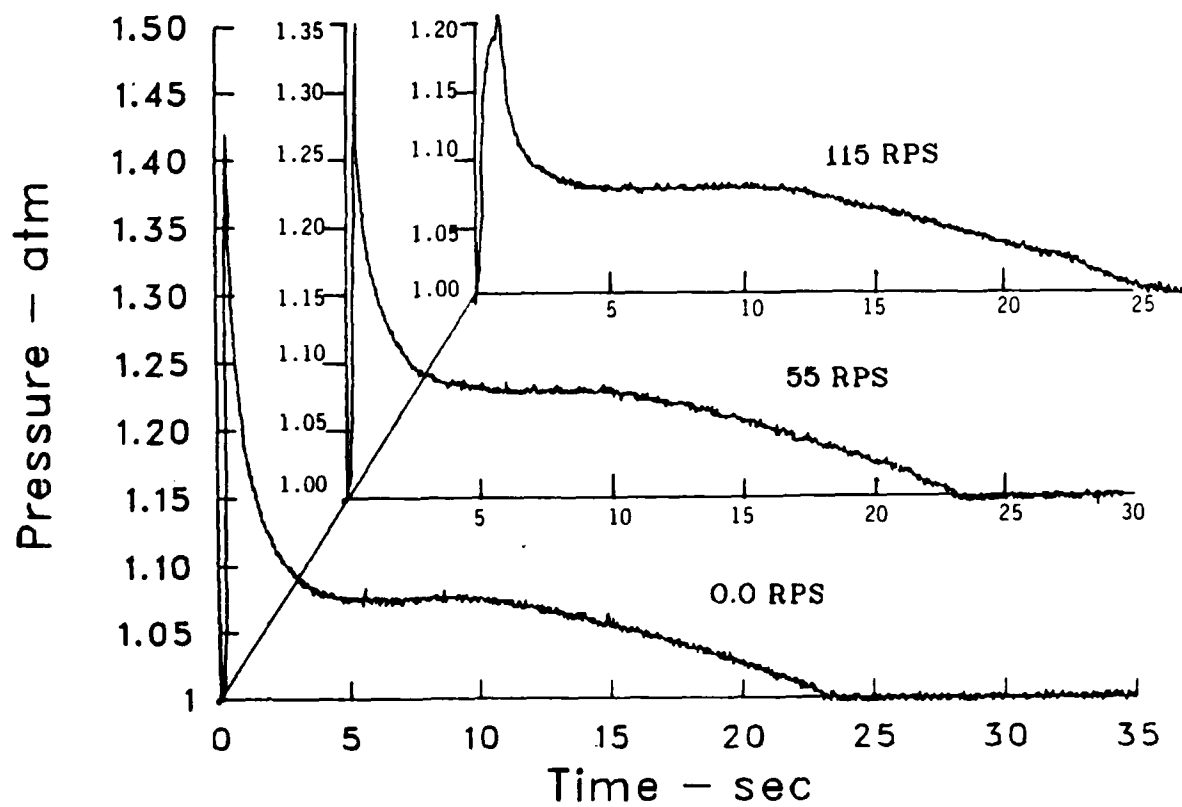


Figure 13. Chamber Pressures for AP-1 Propellant Tests

pass filtered, chamber pressure as a function of time and spin rate. Although Fourier analysis of the signals did not reveal a characteristic frequency of the fluctuations, the pressure fluctuations increase near the end of the propellant burn. There appears (Figure 14) to be a single large pressure fluctuation between 10 and 15 seconds at the four higher spin rates and, currently, there is no explanation for this phenomenon.

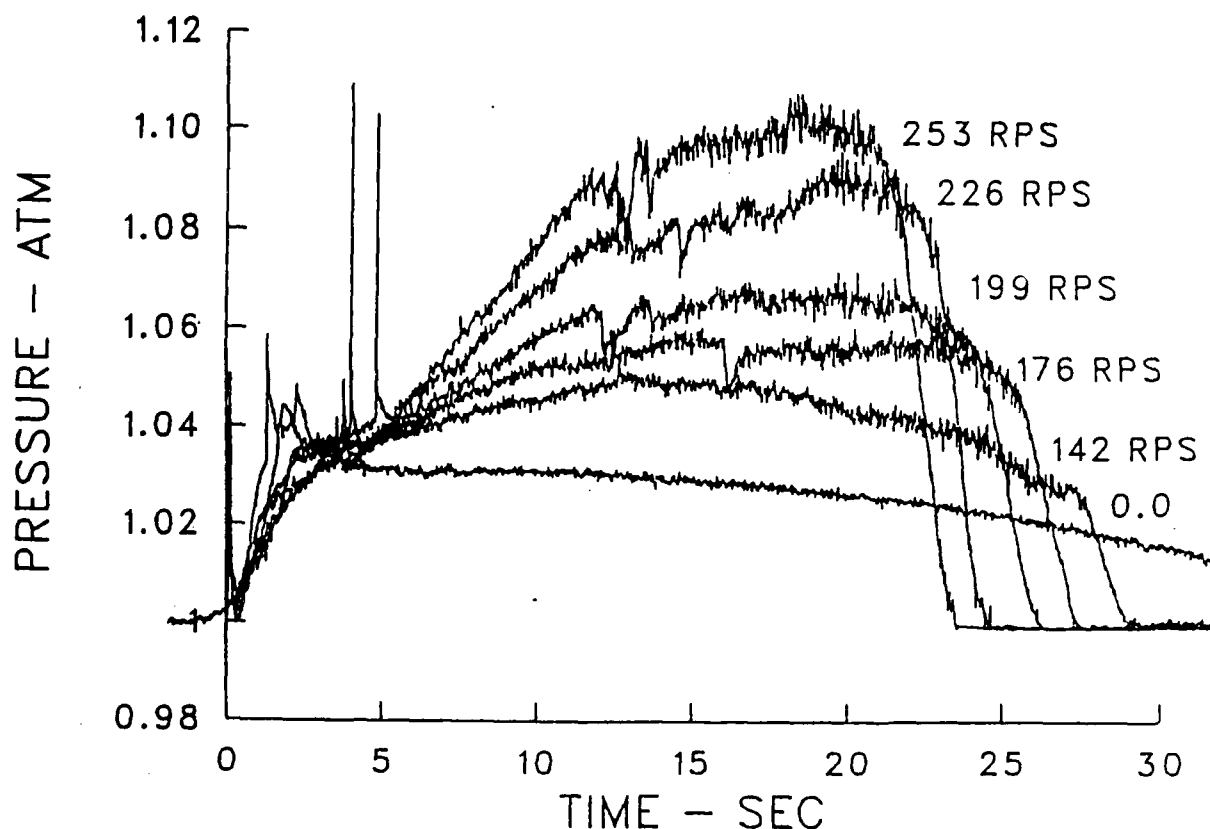


Figure 14. Effects of Spin Rate on Chamber Pressure, AP-2 Propellant

Figure 16 shows the ignition phase of the AP-2 tests. Again, a 20 volt pulse was applied to the electric match at time zero and a pressure pulse from ignition of the external black powder (marked by the letter "A") was clearly detected. A second pulse (marked by the letter "B") corresponds to the burning of black powder that was cemented to the propellant grain. This pulse is longer in duration than the initial pulse, which is expected, but is still in the form of a pulse, indicating that full ignition of the propellant has not yet occurred. The letter "C" designates the approximate location on the pressure history where ignition of the propellant can be detected. The onset of rapid fluctuations of pressure can be seen near this point. The zero spin case is omitted from Figure 16 because it first appeared that that the propellant was not going to ignite; however, after about six seconds, the propellant began to burn vigorously. (For this and other reasons, one gram of black powder was subsequently cemented to the surface of the propellant grain to insure ignition.)

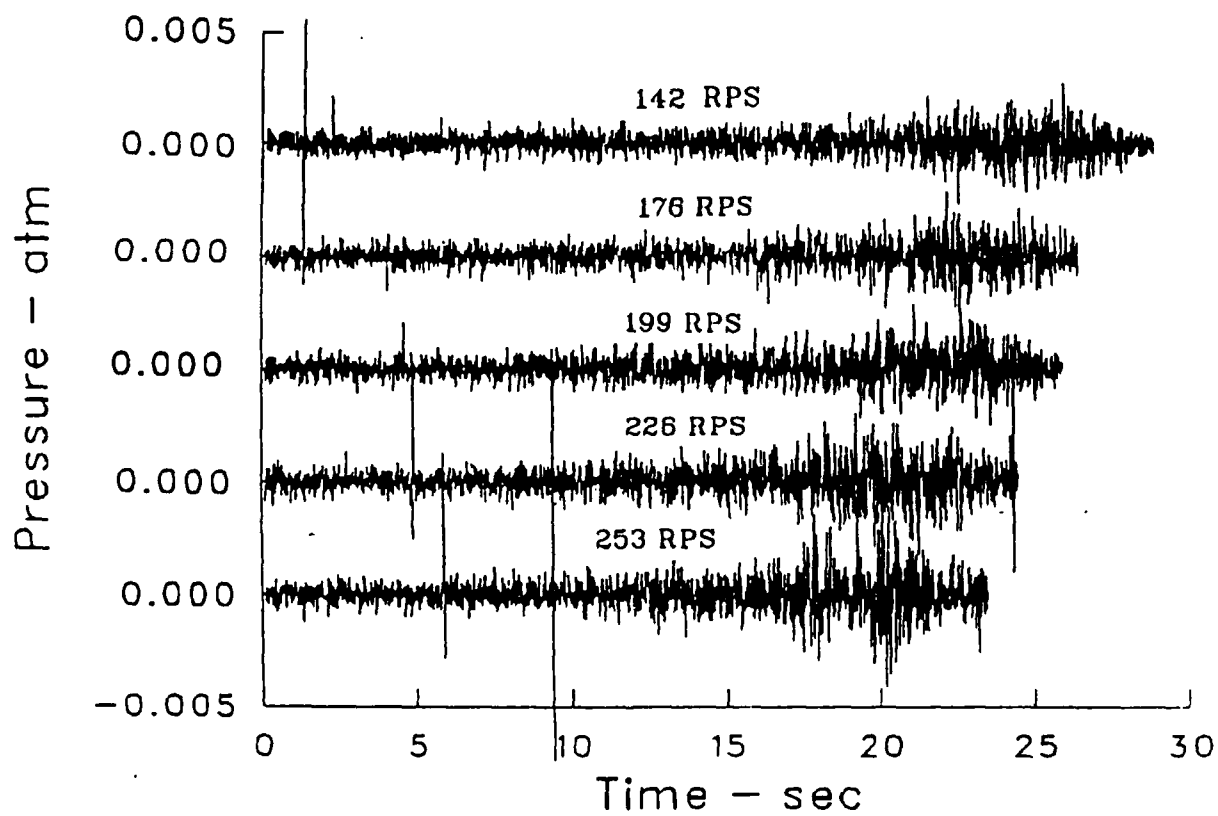


Figure 15. Chamber Pressure Fluctuations, AP-2 Propellant

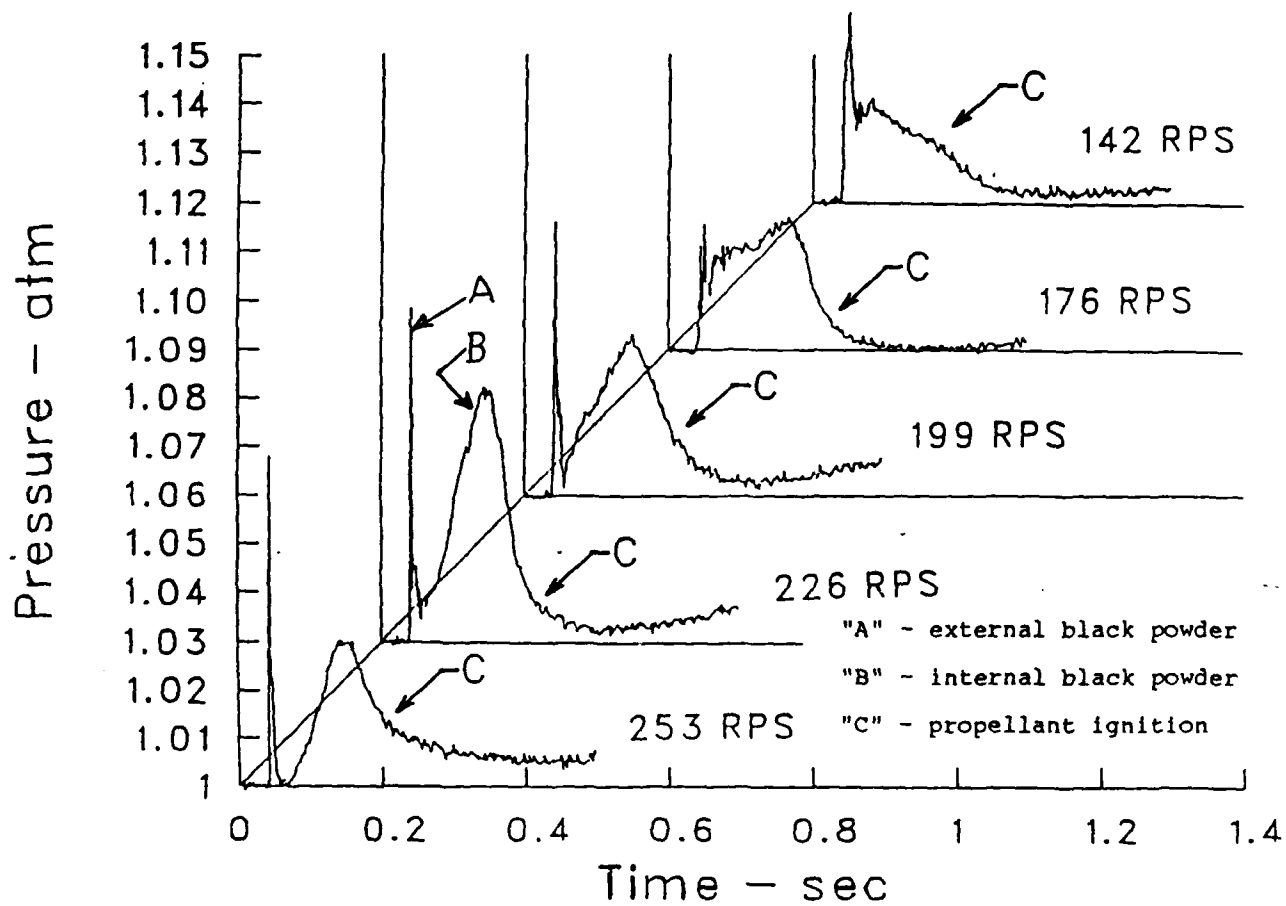


Figure 16. Ignition Phase of Propellant Burn, AP-2 Propellant

Figure 17 shows the first five seconds of the chamber pressure for the AP-2 tests where the magnesium-teflon igniters ignited and burned. The magnesium-teflon igniters were designed to burn for approximately 2 seconds and the two second burn phase could be detected on chamber pressure curves. A distinct pulse in the pressure, believed to occur at burn-out, is preceded by an increase in pressure for about two seconds; this is marked by the letter "D" in four of the five pressure histories. This event in the pressure history has been correlated with an increased brightness of the burning gasses leaving the propellant chamber in the video tapes of the experiments. These pressure distributions, during the first few seconds of burn, do not seem to be effected substantially by the spin rate. Note that there is no correlation between spin rate and the time of ignition nor the the burn rate of the magnesium-teflon igniters.

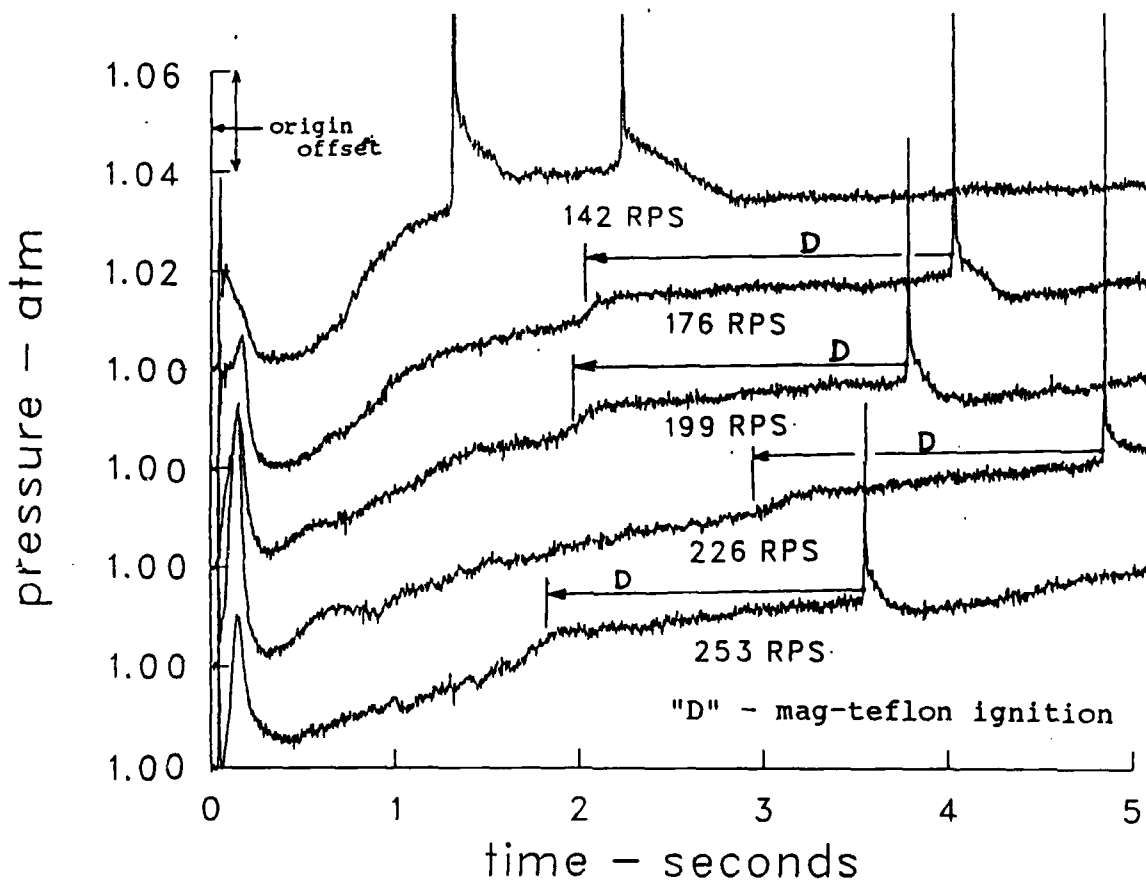
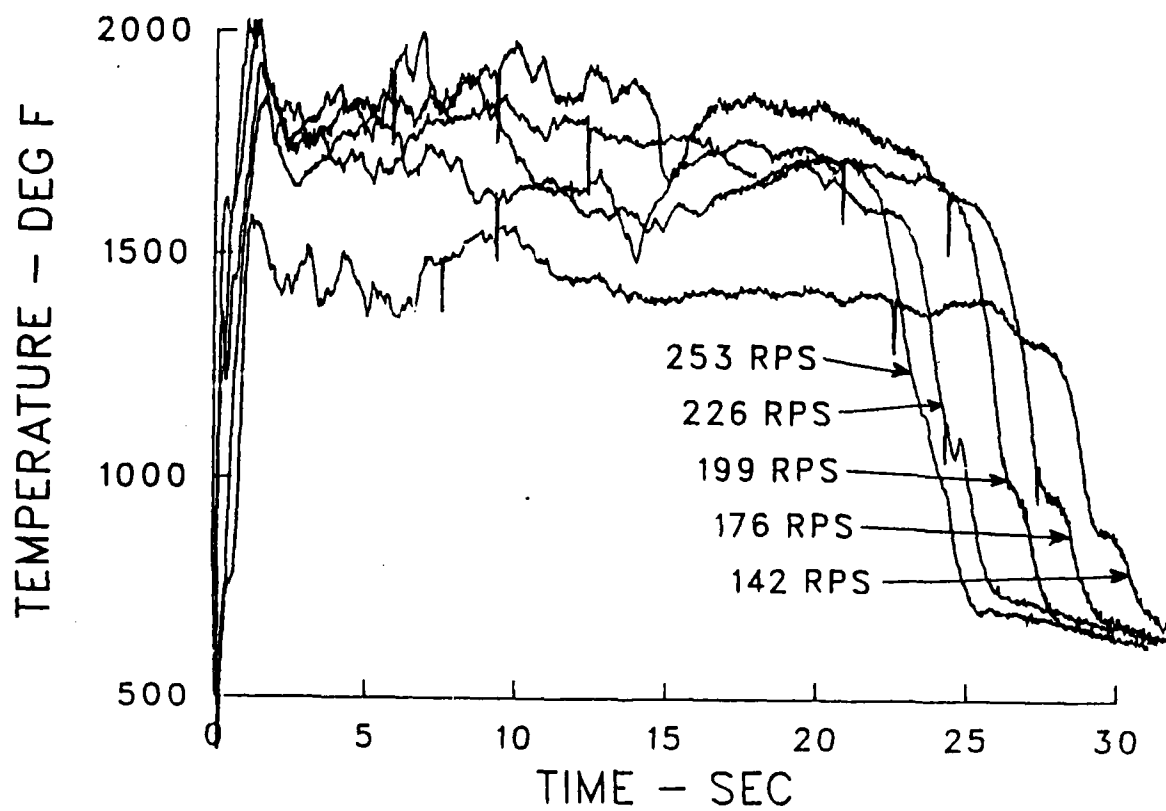


Figure 17. Early Chamber Pressure History, AP-2 Propellant

Figure 18 shows the measured chamber temperatures. These temperatures are believed to be lower than that of the propellant gas. It is speculated that the thermocouple becomes quickly coated with propellant residue which prevents efficient convective heat transfer. The thermocouple is also located close to the igniter housing and the base bulk-head which would adversely affect radiation heat transfer. The thermocouple responds quickly to the ignition phase and also shows a steep gradient at the end of burn and may therefore be useful for determining burn time in free-flight tests.



**Figure 18.** Chamber Temperature Measurements, AP-2 Propellant

## IV. Analysis and Discussion

The results presented here should provide guidance in the formulation of a model for the burning propellant, but this current effort is not intended to include such a model. A brief examination of the data suggests that a number of items could influence the modeling and that a number of parameters may be easily determined or approximated.

The very broad assumption is made that the burn history can be approximated by an equivalent "burn" at a constant chamber pressure. The constant chamber pressure would be less than the maximum value and the length of burn would likely be shorter. Estimates of equivalent "burn time" were made without any significant analytical backing. If the Mach number of the exhausting gas is substantially less than sonic, the incompressible Bernoulli equation provides a reasonable estimate of dynamic pressure in the jet flowing out the propellant chamber. The total pressure ( $p_t$ ) is assumed to be equal to the chamber pressure and the ambient (atmospheric) pressure is assumed to be equal to  $p_s$ :

$$p_t = p_s + \rho v^2/2.$$

The mass flow rate is:

$$\dot{m} = \rho A v$$

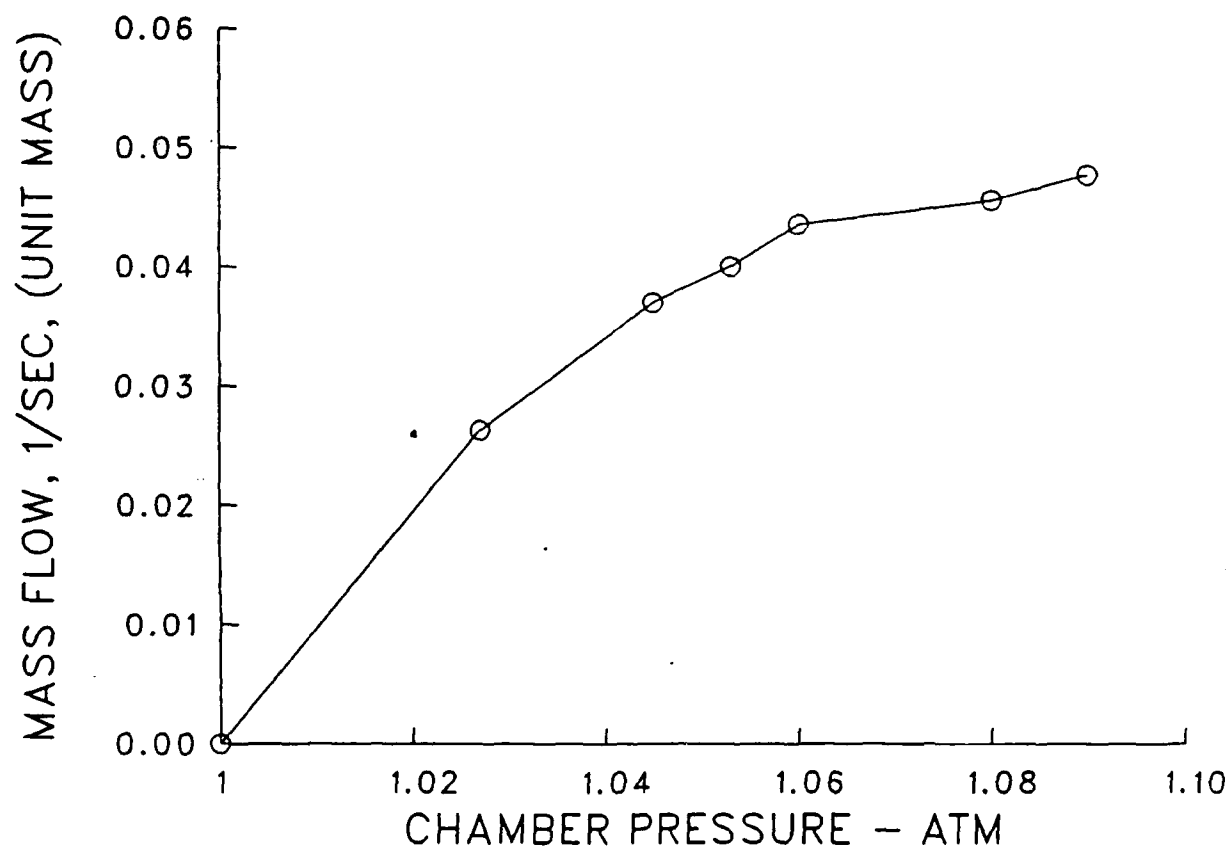
where term  $A$  is the area of the exit hole if a discharge coefficient of 1.0 is assumed. There are now two equations with the two unknowns of  $\rho$  (density) and  $v$  (bulk velocity of the gasses in the jet). The mass flow rate was assumed to be the mass of the propellant grain divided by the length of burn. Table 3 gives the equivalent "burn times" with the densities and velocities determined by the above procedure.

Table 3. Equivalent Burn Time

RPS	$p_t$	$t \uparrow$ (sec)	$\dot{m} \uparrow$	$\rho$ (kg/m <sup>3</sup> )	$v$ (m/sec)
0.0	1.027	38	.0263	.0577	308
142	1.045	27	.0370	.0686	365
176	1.053	25	.0400	.0678	398
199	1.060	23	.0435	.0708	415
226	1.080	22	.0455	.0580	529
253	1.090	21	.0476	.0566	568
$\uparrow t$ represents the equivalent length of burn					
$\uparrow$ unit mass flow rate, i.e. 1.0/t					

Figure 19 shows how the mass flow rate varies with chamber pressure; an increasing chamber pressure corresponds to an increasing spin rate. With this data it would now be possible, for a given "burn," to look at the instantaneous chamber pressure, determine the instantaneous mass flow rate, integrate the mass flow rate as a function of time, and compare the result with known propellant weight.

Figures 20 and 21 show, respectively, the estimated densities and velocities. The densities are not expected to vary too much since the gas temperature of the burning



**Figure 19.** Estimated Mass Flow Rates vs. Measured Chamber Pressure



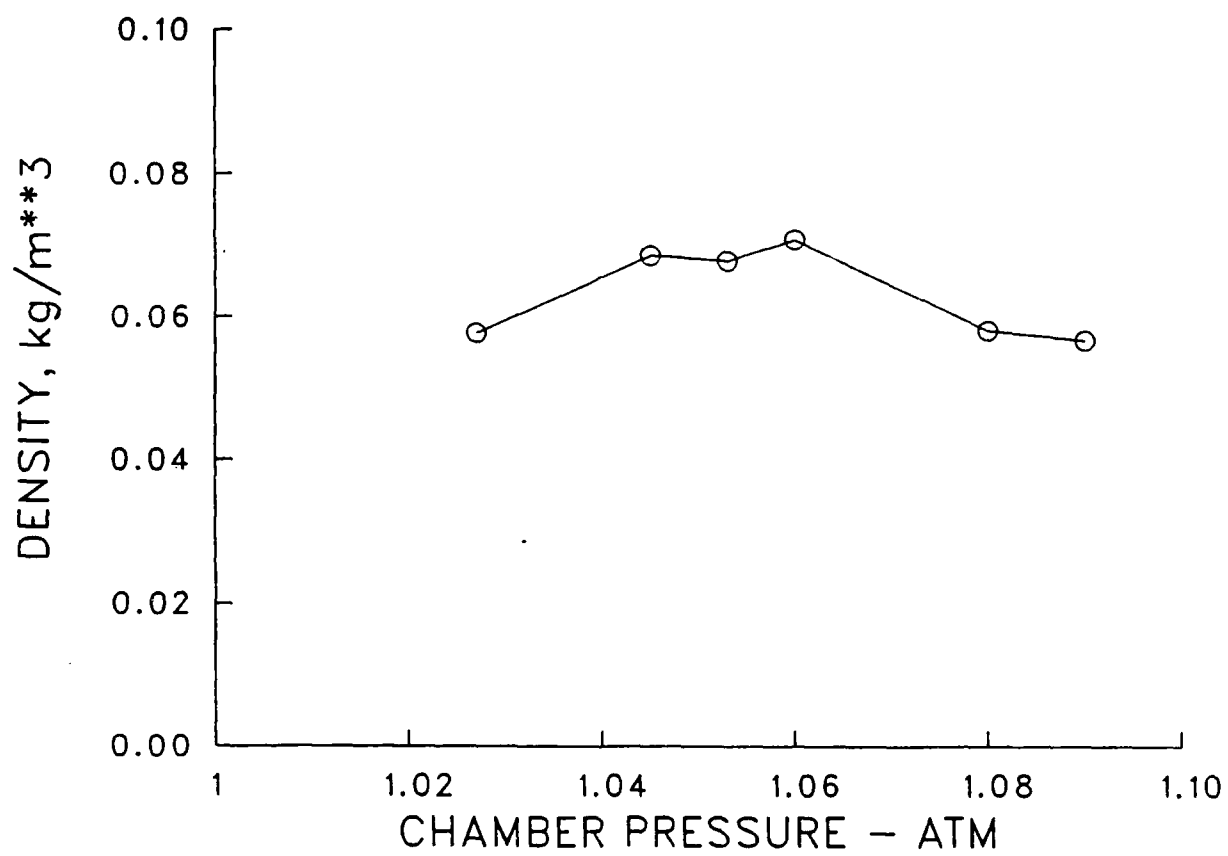


**Figure 20.** Estimated Gas Densities in the Base Throat

propellant should be relatively constant and the chamber pressure changes by only a few percent. The chamber pressure histories, Figure 13, for the two highest spin rates are the most "non-constant" and their equivalent burn times are likely to have the largest error. It does appear that the densities for the two highest spin rates (highest chamber pressures) are too low; this would result from an estimated equivalent burn time that is too long. The velocities of Figure 21 show a monotonic increase with increasing chamber pressure as expected, but the two velocities at the highest pressure appear to be too large. If shorter equivalent burn times were used for the two highest spin rates, the densities would increase, the velocities would decrease, and smoother variations with chamber pressure would result.

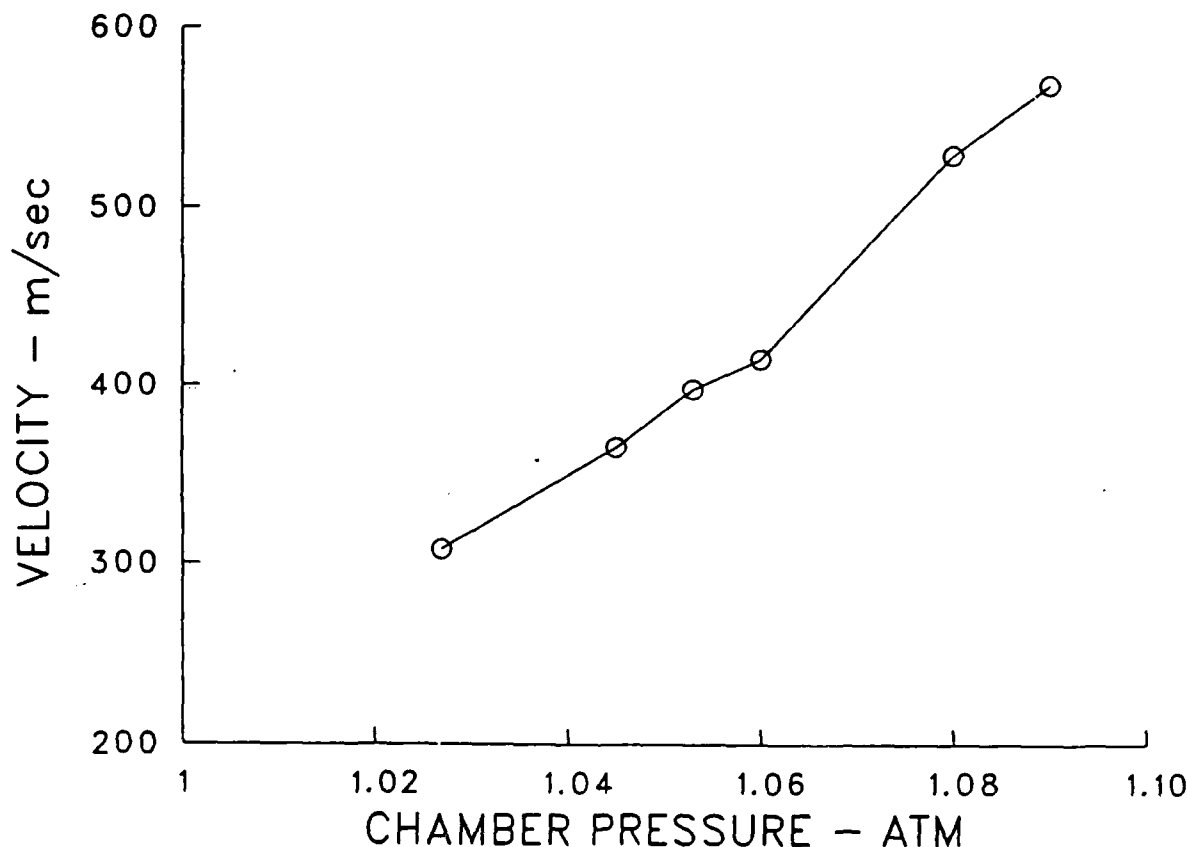


Figure 21. Estimated Throat Velocities

The speed of sound in the gas is not known, but if the temperature is assumed to be 2000° Kelvin and the ratio of specific heats is 1.4, the speed of sound would be 900 meters/sec. The Mach number at higher velocities would be greater than 0.5, but still significantly less than sonic.

Figures 10 and 13 demonstrate the enhanced burning from the higher spin rates; however, the specific enhancement mechanism is not yet well understood. Enhanced burning from increased pressure, due to the centrifugal force of the gas at the highest spin rate, is estimated to increase the burning rate by only 0.25 percent. This is based on the Miller

strand burner tests with varying ambient pressure.

Enhanced burning may be caused by the circumferential flow in the chamber. If a thin layer of gas has just been formed by burning, it will be moving at the same angular rate as the solid propellant. As the layer moves toward the center of the chamber the angular velocity must increase in order to conserve angular momentum. If viscous forces are sufficient, boundary layer type velocity gradients could result in cross flow velocities near the propellant surface, which would increase the burning rate. If these speculations are valid, the circumferential or swirling flow would be small initially. As the surface of the grain recedes, the swirling action would increase and result in higher burning rates.

After the initial pressure rise, for the zero spin case (see Figure 13), the pressure steadily decreases for the entire burn. This qualitative behavior would be expected if the entire surface, including that in the slotted areas, was burning and the surfaces were regressing linearly. Pressure variations with spin are not substantially different for the first 3.5 seconds; but after that, it takes 10 to 15 seconds in order to reach near-maximum pressure. This behavior seems to be consistent with the analysis of the previous paragraph, but other possibilities exist. Burning enhancement may occur only on the central core and not extend into the slotted areas, which would give the relatively long time for pressure to build to the maximum. If the high-g centrifugal forces distort the grain and close off the slotted areas, the surface area for burn would be significantly different.

Starting with the estimated data of Figures 19-21, iterative procedures could be applied until the integrated mass flow rates are equal to the mass of the propellant grain. Velocity, density, and mass flow rates as a function of chamber pressure should be more accurately determined. Similarly, various models for burning surface area could be assumed and iterations made until one model is capable of predicting the experimental pressure-time histories.

## V. Conclusions

- Propellant burn characteristics have been successfully measured.
- Throat velocities are subsonic.
- These experimental results along with the experimental burning rates provide a basis for semi-empirical modeling.
- Tests at simulated altitudes are needed.
- Temperature measurements may be valuable even though they are not accurate.
- Problem areas identified as critical to free-flight testing are location of pressure orifices to avoid plugging and the thermocouple installation for measurement of chamber temperature.

# DISTRIBUTION LIST

<u>No.</u> <u>Copies</u>	<u>Organization</u>	<u>No.</u> <u>Copies</u>	<u>Organization</u>
12	Administrator Defense Technical Information Center ATTN: DTIC-FDAC Cameron Station, Bldg. 5 Alexandria, VA 22304-6145	1	Commander U.S. Army AMCCOM ATTN: SMCAR-CAWS-AM Mr. DellaTerga Picatinny Arsenal, NJ 07806-5000
1	Commander US Army Materiel Command ATTN: AMCDRA-ST 5001 Eisenhower Avenue Alexandria, VA 22333-0001	1	OPM Nuclear ATTN: AMCPM-NUC COL. W. P. Farmer Dover, NJ 07801-5001
1	Commander US Army ARDEC ATTN: SMCAR-TDC Picatinny Arsenal, NJ 07806-5000	1	AFWL/SUL Kirtland AFB, NM 87117-6008
1	Commander U.S. Armament RD&E Center US Army AMCCOM ATTN: SMCAR-MSI Picatinny Arsenal, NJ 07806-5000	3	Commander U.S. Armament RD&E Center US Army AMCCOM ATTN: SMCAR-FSA Mr. F. Brody Mr. R. Botticelli Mr. P. Demasi Picatinny Arsenal, NJ 07806-5000
1	Commander U.S. Armament RD&E Center US Army AMCCOM ATTN: SMCAR-LC Picatinny Arsenal, NJ 07806-5000	2	Commander U.S. Armament RD&E Center US Army AMCCOM ATTN: SMCAR-AET-A Mr. R. Kline Mr. H. Hudgins Picatinny Arsenal, NJ 07806-5000
4	Commander U.S. Army AMCCOM ATTN: AMCPM-CAWS R. Kantenwein J. Williams D. Grubbs R. DeKleine Picatinny Arsenal, NJ 07806-5000	2	Commander U.S. Armament RD&E Center US Army AMCCOM ATTN: SMCAR-AET Mr. F. Scerbo Mr. J. Bera Picatinny Arsenal, NJ 07806-5000

# DISTRIBUTION LIST

<u>No.</u> <u>Copies</u>	<u>Organization</u>	<u>No.</u> <u>Copies</u>	<u>Organization</u>
1	Commander US Army Armament, Munitions and Chemical Command ATTN: AMSMC-IMP-L Rock Island, IL 61299-7300	10	C. I. A. OIC/DB/Standard GE47 HQ Washington, DC 20505
1	Commander U.S. AMCCOM ARDEC CCAC Benet Weapons Laboratory ATTN: SMCAR-CCB-TL Watervliet, NY 12189-4050	1	Commandant US Army Infantry School ATTN: ATSH-CD-CS-OR Fort Benning, GA 31905-5400
1	Commander US Army Aviation Systems Command ATTN: AMSAV-ES 4300 Goodfellow Blvd St Louis, MO 63120-1789	1	Commander US Army Missile Command Research Development and Engineering Center ATTN: AMSMI-RD Redstone Arsenal, AL 35898-5230
1	HQDA DAMA-ART-M Washington, DC 20310	1	Commander US Army Missile Command ATTN: AMSMI-RDK, Mr. Dahlke Redstone Arsenal, AL 35898-5230
1	Director US Army Aviation Research and Technology Activity Moffett Field, CA 94035-1099	1	Director US Army Missile and Space Intelligence ATTN: AIAMS-YDL Redstone Arsenal, AL 35898-5500
1	Commander US Army Communications Electronics Command ATTN: AMSEL-ED Fort Monmouth, NJ 07703-5000	1	Commander US Army Tank Automotive Command ATTN: AMSTA-TSL Warren, MI 48397-5000
1	Commander CECOM R&D Technical Library ATTN: AMSEL-IM-L, (Reports Section) B. 2700 Fort Monmouth, NJ 07703-5000	1	Director US Army TRADOC Analysis Center ATTN: ATOR-TSL White Sands Missile Range NM 88002-5502

# DISTRIBUTION LIST

<u>No.</u> <u>Copies</u>	<u>Organization</u>	<u>No.</u> <u>Copies</u>	<u>Organization</u>
1	Commander US Army Development & Employment Agency ATTN: MODE-ORO Fort Lewis, WA 98433-5000	1	Commander Naval Surface Weapons Center ATTN: Dr. W. Yanta Aerodynamics Branch K-24, Building 402-12 White Oak Laboratory Silver Spring, MD 20910
1	Commandant US Army Field Artillery School ATTN: ATSF-GD Fort Sill, OK 73503	1	Director National Aeronautics and Space Administration Ames Research Center ATTN: Dr. J. Steger Moffet Field, CA 94035
1	Director US Army Field Artillery Board ATTN: ATZR-BDW Fort Sill, OK 73503	1	University of Santa Clara Department of Physics ATTN: R. Greeley Santa Clara, CA 95053
1	Commander US Army Dugway Proving Ground ATTN: STEDP-MT Mr. G. C. Travers Dugway, UT 84022	1	Arizona State University Department of Mechanical and Energy Systems Engineering ATTN: G.P. Neitzel Tempe, AZ 85281
1	Commander US Army Yuma Proving Ground ATTN: STEYP-MTW Yuma, AZ 85365-9103	1	Director Lawrence Livermore National Laboratory ATTN: Mail Code L-35 Mr. T. Morgan P.O. Box 808 Livermore, CA 94550
2	Director Sandia National Laboratories ATTN: Dr. W. Oberkampf Dr. W. P. Wolfe Division 1636 Albuquerque, NM 87185	1	Commander Defense Advanced Research Projects Agency ATTN: MAJ. R. Lundberg 1400 Wilson Blvd. Arlington, VA 22209
1	Air Force Armament Laboratory ATTN: AFATL/DLODL (Tech Info Center) Eglin AFB, FL 32542-5438		

## DISTRIBUTION LIST

### Aberdeen Proving Ground

Director, USAMSAA

ATTN: AMXSY-D

AMXSY-RA, R. Scungio

Commander, USATECOM

ATTN: AMSTE-SI-F

AMSTE-TE-F, W. Vomocil

PM-SMOKE, Bldg. 324

ATTN: AMCPM-SMK-M

Mr. J. Callahan

Commander, CRDC, AMCCOM

ATTN: SMCCR-MU

Mr. W. Dee

Mr. C. Hughes

Mr. D. Bromley

ATTN: SMCCR-RSP-A

Mr. Miles Miller

Mr. Donald Olson

ATTN: SMCCR-SPS-IL

SMCCR-RSP-A

SMCCR-MU

# USER EVALUATION SHEET/CHANGE OF ADDRESS

This Laboratory undertakes a continuing effort to improve the quality of the reports it publishes. Your comments/answers to the items/questions below will aid us in our efforts.

1. BRL Report Number \_\_\_\_\_ Date of Report \_\_\_\_\_
2. Date Report Received \_\_\_\_\_
3. Does this report satisfy a need? (Comment on purpose, related project, or other area of interest for which the report will be used.) \_\_\_\_\_  
\_\_\_\_\_  
\_\_\_\_\_
4. How specifically, is the report being used? (Information source, design data, procedure, source of ideas, etc.) \_\_\_\_\_  
\_\_\_\_\_  
\_\_\_\_\_
5. Has the information in this report led to any quantitative savings as far as man-hours or dollars saved, operating costs avoided or efficiencies achieved, etc? If so, please elaborate. \_\_\_\_\_  
\_\_\_\_\_  
\_\_\_\_\_
6. General Comments. What do you think should be changed to improve future reports? (Indicate changes to organization, technical content, format, etc.) \_\_\_\_\_  
\_\_\_\_\_  
\_\_\_\_\_

CURRENT ADDRESS	_____
	Name
	_____
	Organization
	_____
	Address
	_____
	City, State, Zip

7. If indicating a Change of Address or Address Correction, please provide the New or Correct Address in Block 6 above and the Old or Incorrect address below.

OLD ADDRESS	_____
	Name
	_____
	Organization
	_____
	Address
	_____
	City, State, Zip

(Remove this sheet, fold as indicated, staple or tape closed, and mail.)



----- FOLD HERE -----

Director  
U.S. Army Ballistic Research Laboratory  
ATTN: SLCBR-DD-T  
Aberdeen Proving Ground, MD 21005-5066

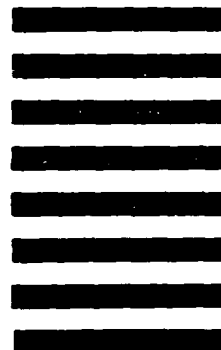


NO POSTAGE  
NECESSARY  
IF MAILED  
IN THE  
UNITED STATES

OFFICIAL BUSINESS  
PENALTY FOR PRIVATE USE, \$300

**BUSINESS REPLY MAIL**  
FIRST CLASS PERMIT NO 12062 WASHINGTON, DC  
POSTAGE WILL BE PAID BY DEPARTMENT OF THE ARMY

Director  
U.S. Army Ballistic Research Laboratory  
ATTN: SLCBR-DD-T  
Aberdeen Proving Ground, MD 21005-9989



----- FOLD HERE -----